CALT-68-1898
DOE RESEARCH AND
DEVELOPMENT REPORT

CALT-68-1898

# CENTRAL DRIFT CHAMBER TRACKING AT A TAU-CHARM FACTORY*

*Alan J. Weinstein*
California Institute of Technology
256-48 Lauritsen Lab, Pasadena, CA 91125, USA

FERMILAB
OCT 72 1990
LIBRARY

**Abstract**

**Several design issues relevant to the design of a central tracking system for a $\tau c$F are discussed, including light gases, cell geometry, and detector uniformity/hermeticity.**

Fermilab Library
0 1160 0031965 1

## 1 INTRODUCTION

To maximize the physics output of a $\tau c$F, we want to build the best possible central tracking system, within the constraints imposed by the rest of the detector and interaction region: the minimum and maximum radius and polar-angle coverage available to the tracking system. The overall design philosophy for a $\tau c$F drift chamber was described in Ref. [1]. Here we only describe progress since the 1989 workshop in some specific details of the design, so the reader should refer to Ref. [1] for the overall picture.

There are several paths to improvement on previous drift chamber designs:

- reduce multiple scattering: thin walls, light gas, light wires (multiple scattering dominates momentum resolution at a $\tau c$F)
- cell design: best hit efficiency, uniform time-to-distance relation (TDR) and dE/dx collection region
- "cool" gas for lowest diffusion, best hit resolution
- superlayer layout: simple, efficient pattern recognition and triggering
- endplate design: maximize $|\cos\theta|$ coverage, precise wire positioning, embedded connections to minimize cabling difficulties

We will discuss progress in some of these issues in the following sections.

Because of rather limited activity (or interest) in central tracking during this workshop, this report cannot discuss progress made by the $\tau c$F community; instead, we draw on work done by the larger HEP community. The only other contribution to the tracking discussions was made by the Sevilla group, which is building a full GEANT simulation of the $\tau c$F detector. They have already completed several studies relevant to tracking using this program, and the reader is referred to their contributions to these proceedings.

*Work supported in part by the U.S. Dept. of Energy under Grant No. DE-FG03-92-ER40701.

## 2 LIGHT DRIFT CHAMBER GASES

Much progress has been made in the development of light drift chamber gases (primarily helium-based) in the context of drift chamber designs for an asymmetric $B$ Factory (ABF). Light gases reduce multiple scattering (which is more important at a $\tau c$F than at an ABF). They also minimize noise hits produced by the absorption of synchrotron radiation photons accompanying high-current $e^{\pm}$ beams in the storage ring.

To make a useful drift chamber gas, other gases are added to the helium. To provide more ionization for improved resolution and dE/dx measurements, one can add up to 7% isobutane (any more is flammable). Additional ionization, quenching, and reduced diffusion (cooling) can be obtained by adding 10% $CO_2$ or 20-30% DME. The properties of common drift chamber gases and gas mixtures are given in Table 1. Prototype gas studies have been performed at SLAC [2, 3], ETH&PSI [4], KEK [5], Dortmund [6], and Heidelberg [7].

Table 1: Properties of drift chamber gases (from Ref. [2]).

| Gas Mixture | Ratio | $X_0$ [m] | $N_P$ [cm$^{-1}$] |
|---|---|---|---|
| Helium | 100:0 | 5284 | 4.2 |
| Argon | | 110 | 24.3 |
| $CO_2$ | | 183 | 36.5 |
| $C_2H_6$ | | 340 | 51 |
| $iC_4H_{10}$ | | 169 | 93 |
| DME ($C_2H_6O$) | | 222 | 62 |
| Ar:$C_2H_6$ | 50:50 | 166 | 37.7 |
| $CO_2$:$iC_4H_{10}$ | 90:10 | 181 | 42.2 |
| He:$iC_4H_{10}$ | 90:10 | 1313 | 13.1 |
| | 80:20 | 749 | 22.0 |
| | 70:30 | 524 | 30.8 |
| He:$CO_2$:$iC_4H_{10}$ | 80:10:10 | 776 | 16.3 |
| | 70:20:10 | 550 | 19.5 |
| He:DME | 90:10 | 1612 | 10.0 |
| | 80:20 | 951 | 15.8 |
| | 70:30 | 674 | 21.5 |

Even with these additives, a mixture like He, 10% $CO_2$, 7% $C_4H_{10}$ has 29 ion pairs per cm, as compared with HRS gas ($Ar/CO_2/CH_4$) with 93 ip/cm. Despite this, the pulse height is as large as in HRS gas (Fig. 1), due to a higher gas gain and the Penning effect, in which an excited (but not ionized) helium atom transfers its energy to the a more easily ionized additive ($He^* + A \rightarrow He + A^+ + e$). Thus, one can achieve 100% hit efficiency using the same operating voltages one would use with HRS gas.

The drift velocity for helium-based gases is not saturated, but rather depends sensitively on the applied electric field and the gas pressure (in the ratio E/P; see Fig. 2). This requires tight monitoring and control of the temperature, pressure, and applied voltages. Even so, the time-to-distance relation (TDR) in a typical drift cell will be non-trivial and will require careful calibration. These are not fundamental problems; many drift

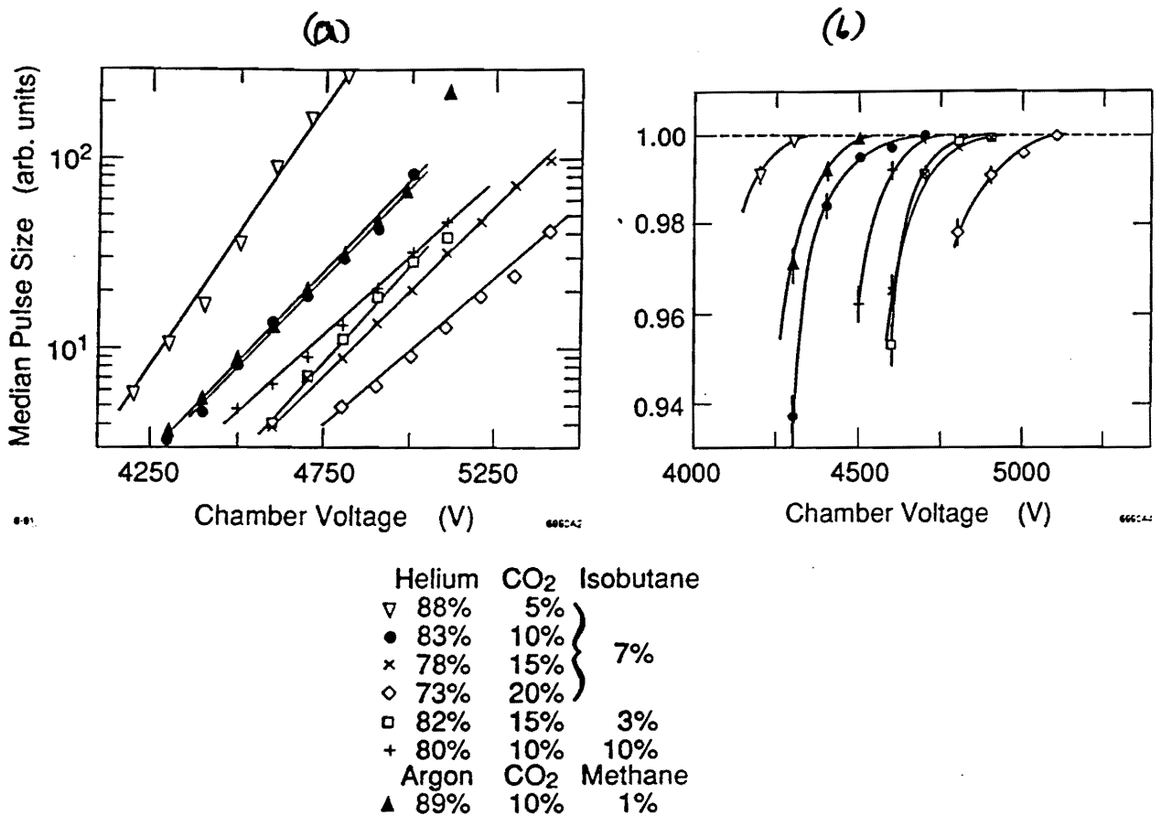


Figure 1: (a) Median pulse height, and (b) single wire efficiency as a function of chamber voltage, for various gases (from Ref. [2]).

chambers operate well with unsaturated gases.

The drift velocity for these gases is somewhat lower than for HRS gas. One advantage of this is that there is less demand for precision TDCs; but for a given cell size, the total drift time is longer, so that more front-end memory is needed, and the trigger information will be longer in arriving. The lower drift velocity also leads to a smaller Lorentz angle $\tan\theta = \kappa vB/E$ in the drift trajectory, resulting in a more uniform TDR and dE/dx collection region.

The bottom line is that the position resolution achievable with helium based gas mixtures is as good or better than that obtained with more conventional gases. This is illustrated in Fig. 3.

### 2.1 He/DME mixtures

Instead of $CO_2$ and isobutane, DME can function as a quencher and a source of ionization [4]. DME is more thermal; there will be less diffusion and thus better spatial resolution. It also has a smaller synchrotron photon absorption cross-section, so there will be fewer salt-and-pepper hits from that source. These mixtures have excellent position resolution; see Fig. 4.

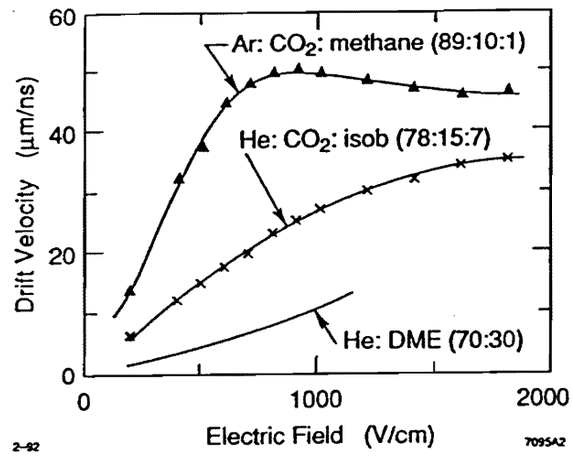


Figure 2: Drift velocity versus electric field in cell for different gases. The drift velocity of Ar:$CO_2$:isob is saturated in the range 700-1000 V/cm (from Ref. [2]).

DME has a slower drift velocity, so more memory is required on the electronics, and there may be more of a pile-up problem. The most serious concern about DME is that it appears to be more susceptible to HV breakdown than He-$CO_2$-$C_4H_{10}$; some afterpulsing has been seen [3].

## 2.2 dE/dx Resolution

The sampling of specific ionization (dE/dx) in the drift chamber gas provides valuable information for particle identification. The dE/dx resolution can be parameterized as:

$$\sigma = 34 N_{samp}^{-0.46} \left(6.83\beta^2 Z/I\right)^{-0.32} (xP)^{-0.32} \tag{1}$$

where $N_{samp}$ is the number of samples, $x$ is the thickness of each sample, $\beta$ is the particle velocity, $Z$ is the atomic number and $I$ the ionization potential (properties of the gas), and $P$ is the gas pressure.

For a given drift chamber gas, the best resolution is obtained when there are lots of samples, and when the entire path length is utilized. This last criterion is relevant when choosing the cell geometry (see below).

The gas-dependent quantity, $Z/I$, is 0.18 for Argon:Ethane and 0.17 for He:DME. Thus, there is not much variation amongst the gas mixtures usually considered for drift chambers. One expects the dE/dx resolution for light gases to be as good as that for conventional gases.

The figure-of-merit for particle identification (especially $e - \pi$ separation) in the momentum region relevant in a $\tau c$F is the average dE/dx pulse height in the relativistic rise region (occupied by $e^{\pm}$) divided by the pulse height for minimum-ionizing particles (*e.g.*, $\sim$ 1 GeV/c $\pi^{\pm}$), then divided by the resolution. The mean dE/dx measured in helium-based gases is illustrated in Fig. 5.

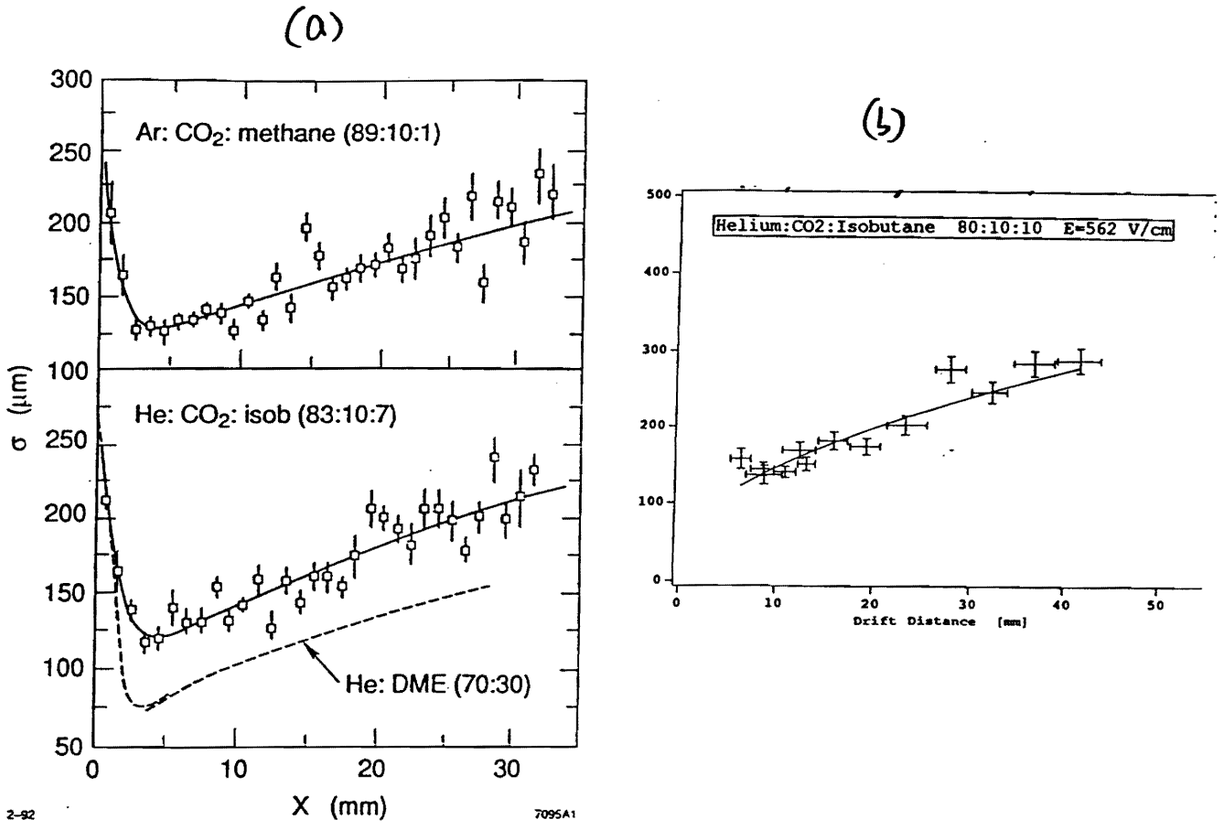


Figure 3: Position resolution in test chamber versus drift distance, showing the effects of ionization statistics close to the wire and diffusion far from the wire in degrading resolution. (a) Ref. [2]; (b) Ref. [4].

### 2.3 Wire Material

In addition to using light gases, it is important to minimize the material in the wires. Depending on the cell geometry, a track will often hit a wire and scatter significantly. Such effects should be included in a realistic simulation of track finding efficiency and momentum resolution, because such scatters will produce significant tails in an otherwise Gaussian detector response.

Light field wires made of carbon fiber, magnesium, or aluminum have been considered (and used). Such materials are strong and lighter than conventional copper. Their use reduces the number of radiation lengths in the tracker, thus reducing the amount of multiple scattering for charged particles and preconversions for photons (see Table 2). They have less gravitational sag, requiring less tension and therefore thinner chamber endplates. Unfortunately, there has been little experience in existing drift chambers with any but Au-plated aluminum (CLEO, AMY, SLD). CLEO and SLD have observed a lessening of the tension on the aluminum wires over time, due to "creep" through the feedthrough crimps; but other groups have not observed this problem [5].

The total number of radiation lengths in a $B$ Factory drift chamber for three different gas/wire combinations is given in Table 2.

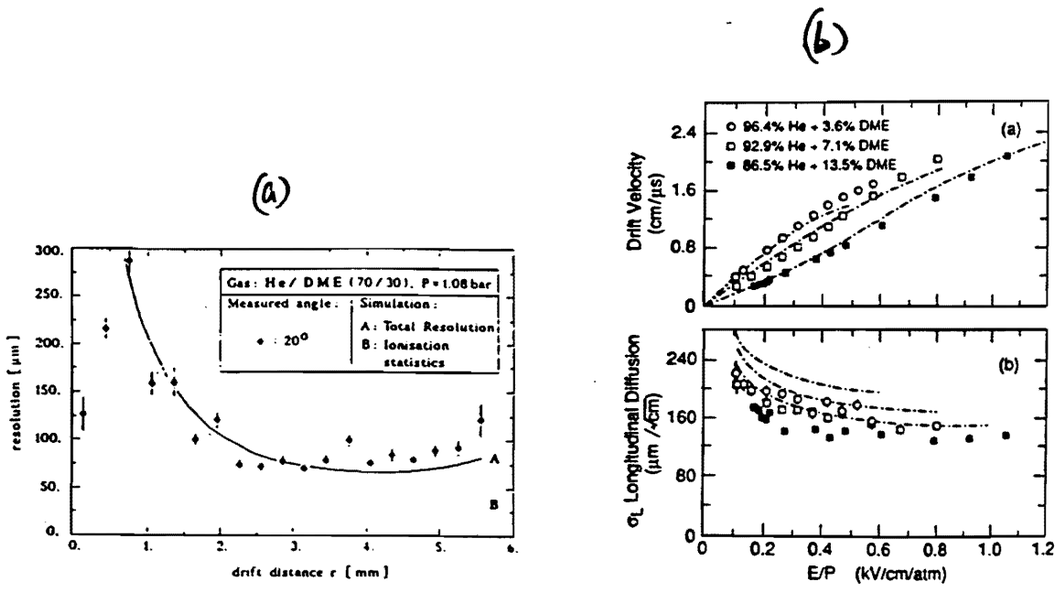


Figure 4: Position resolution in He/DME versus drift distance. (a) Ref. [6]; (b) Ref. [3].

## 2.4 Endplates

The traditional cylindrical drift chamber has the disadvantage of non-uniform response for track trajectories at small angle with respect to the beam. When the track exits through the endplate, one loses hits at large radii, the track finding efficiency and momentum resolution suffers, and the thick endplate introduces undesirable material in front of the endcap calorimeter. More than one $e^+e^-$ experiment has abandoned the hope of doing physics with tracks and photons in the endcap region of the detector because of these problems. Since the physics goals of a $\tau c$F demand the highest precision, solid angle coverage, and hermeticity, the endcap region requires careful attention.

More coverage can be obtained by making the chamber longer (requiring a larger and more expensive crystal calorimeter), but the chamber must fit around the micro-beta quadrapole magnets which will be quite close to the interaction region at a $\tau c$F. The envelope of the micro-beta quads define a stay-clear region in $|\cos\theta|$, of about 0.95. Thus, the obvious geometry of a drift chamber endplate is conical; one keeps beyond the stay-clear while ensuring that no particles within $|\cos\theta| < 0.95$ need pass through an endplate. Conical endplates are also stronger, in principle. The problem is that conical endplates are more difficult to engineer and machine, and it may be more difficult to build them to the required precision. These are not fundamental problems, but they must be weighed against the advantages.

The current design of the $\tau c$F drift chamber endplate is shown in Fig. 6. At present, the endplate is envisioned as a series of steps following the $|\cos\theta| < 0.95$ stay-clear, until a radius of about 48 cm, beyond which the endplate is flat. In other words, a compromise.

Another nice innovation is to build HV, signal, and wire feedthrough connections into multilayer PC-boards which could be glued on to the endplate (as in the H1 drift chamber) or actually form the endplate itself. This makes stringing and cabling much

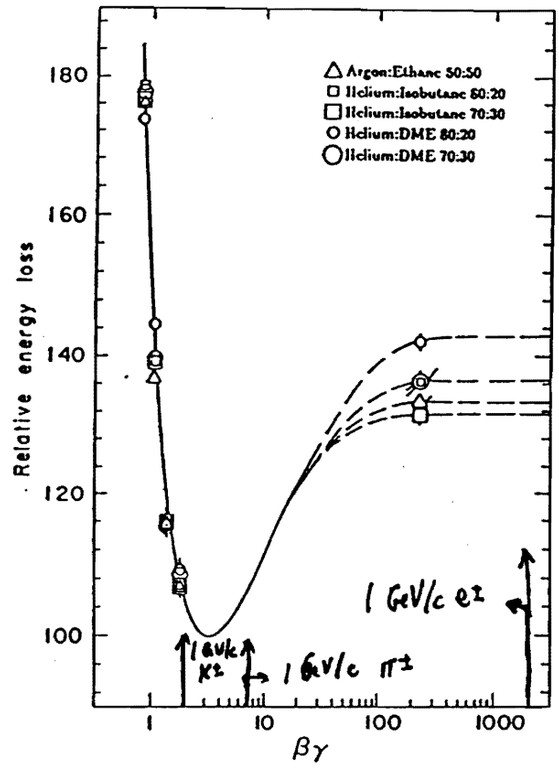


Figure 5: Relative dE/dx energy loss versus $\beta\gamma$ of incident particle, with measurements from Ref. [4].

easier and less error-prone, makes access to the feedthroughs much easier, and (if done right) can reduce the amount of material in the endplate and make the connections more robust. It would, presumably, be more difficult to engineer such a system with a conical endplate.

### 2.5 Small-Angle Stereo Wires

Small-angle stereo wires can achieve adequate $z$-resolution for $\tau c$F physics goals, as long as there are enough layers. One can consider $z$ cathodes in the chamber inner and outer cylindrical walls, but this increases their thickness; thus, one might only put them on the outer walls.

## 3 JET CELL VERSUS SMALL CELL

The drift chamber cell design outlined in Ref. [1] was a jet cell, arranged in superlayers. Since that time, much thought and work has gone into the optimal cell geometry for a $B$ Factory, which is directly relevant for a $\tau c$F as well.

Here I only present a list of pros and cons for jet cells (Fig. 7) versus small cells

Table 2: The total number of radiation lengths in a $B$ Factory drift chamber for three different gas/wire combinations (from Ref. [2]).

| | Number of Radiation Lengths | | |
|---|---|---|---|
| | Case A | Case B | Case C |
| 6,800 20-$\mu$m sense wires: | 0.00020 (tungsten) | 0.00020 (tungsten) | 0.00020 (tungsten) |
| 36,680 55-$\mu$m field wires | 0.00195 (copper) | 0.0031 (aluminum) | 0.00019 (magnesium) |
| 5-$\mu$inch gold plating on field wires | 0.00006 | 0.00006 | 0.00006 |
| gas | 0.0043 (HRS) | 0.00061 (93% He, 10% $CO_2$, 7% isobutane) | 0.00050 (80% He, 20% DME) |
| TOTAL | 0.0070 | 0.0012 | 0.00095 |

(Fig. 8), and suggest that the matter is still very much open to debate and study by the $\tau c$F community.

### 3.1 Pros for small cells

- Smaller cells means shorter drift distance, thus less diffusion and better spatial resolution.
- Small cells means more sense wires. Each wire sees less deposited charge over its lifetime, thus less aging.
- shorter drift distance means shorter memory required on the front-end or readout electronics, and faster trigger decision.
- Jet cell superlayers are typically isolated from one another by "guard" wires, which have complicated electrostatics and therefore are not instrumented as sense wires. These guard wires take up radial space, making it effectively dead. With small cells, one can achieve full path length sampling, and thus better dE/dx resolution.
- Wires in jet cells are close to one another, and they experience stronger electrostatic forces. They thus must be strung under higher tension, requiring thicker endplates than small-cell designs.
- Wires in small cells are typically strung through separate feedthroughs, while wires in jet cells are typically strung through multi-wire feedthroughs. Which kind of

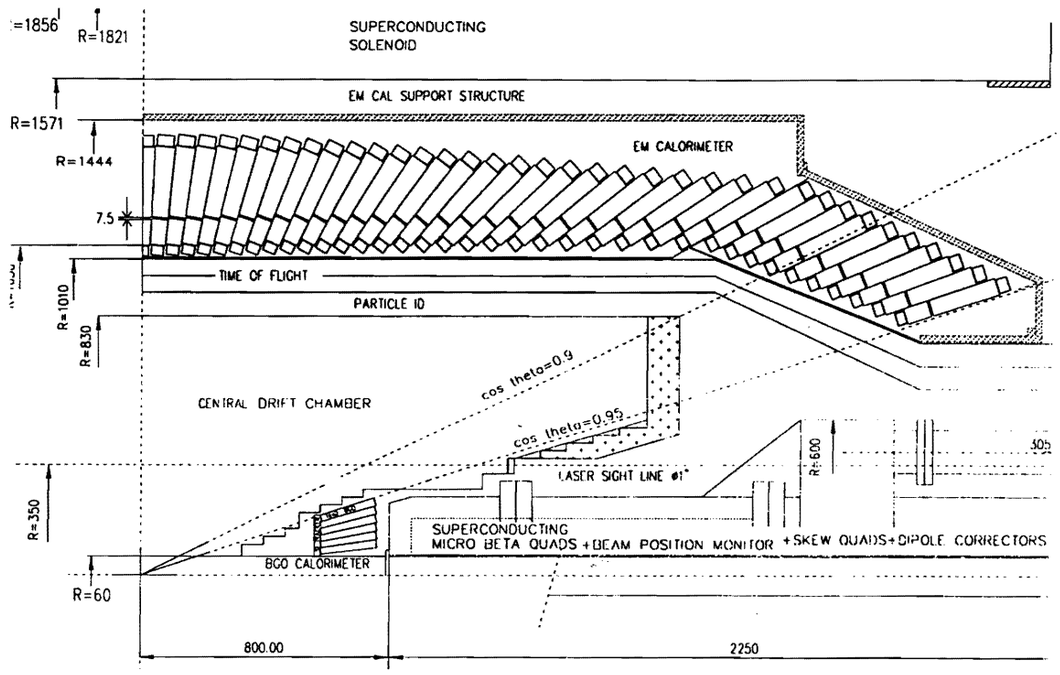


Figure 6: Current schematic of $\tau c$F detector design. Note the drift chamber endplates.

feedthrough provides a better seal depends on the details of the design. But errors in multi-wire feedthrough placement can introduce correlations in the position errors of hits on a track trajectory, which result in a degraded momentum resolution.

- Smaller cells means more field wires to serve as cathodes. For a given drift electric field, this means less charge on each field wire. The field on the surface of a field wire must be kept below some maximum ($\sim$ 20 KV/cm) to avoid whisker growth. So less charge means the wires can be made thinner. Twice as many wires means each wire need only be half as thick; that *halves* the material in wires and also reduces the needed tensioning and therefore the endplate thickness.

### 3.2 Pros for jet cells

- The great advantage of jet cells is that it provides a natural wire grouping for pattern recognition, left/right ambiguity resolution, triggering, and cabling.
- Jet cells provide a more uniform dE/dx collection region, simpler time-distance relation, smaller Lorentz angle; thus it is easier to calibrate and keep in calibration.
- Jet cells have more uniform drift collection region, no "corners" as in small square cells: one avoids long collection times and lowered efficiency in the corners.
- Jet cells provide natural groupings of axial and stereo layers. Since one needs some radial spacing between axial and stereo layers due to stereo "sag", these groupings

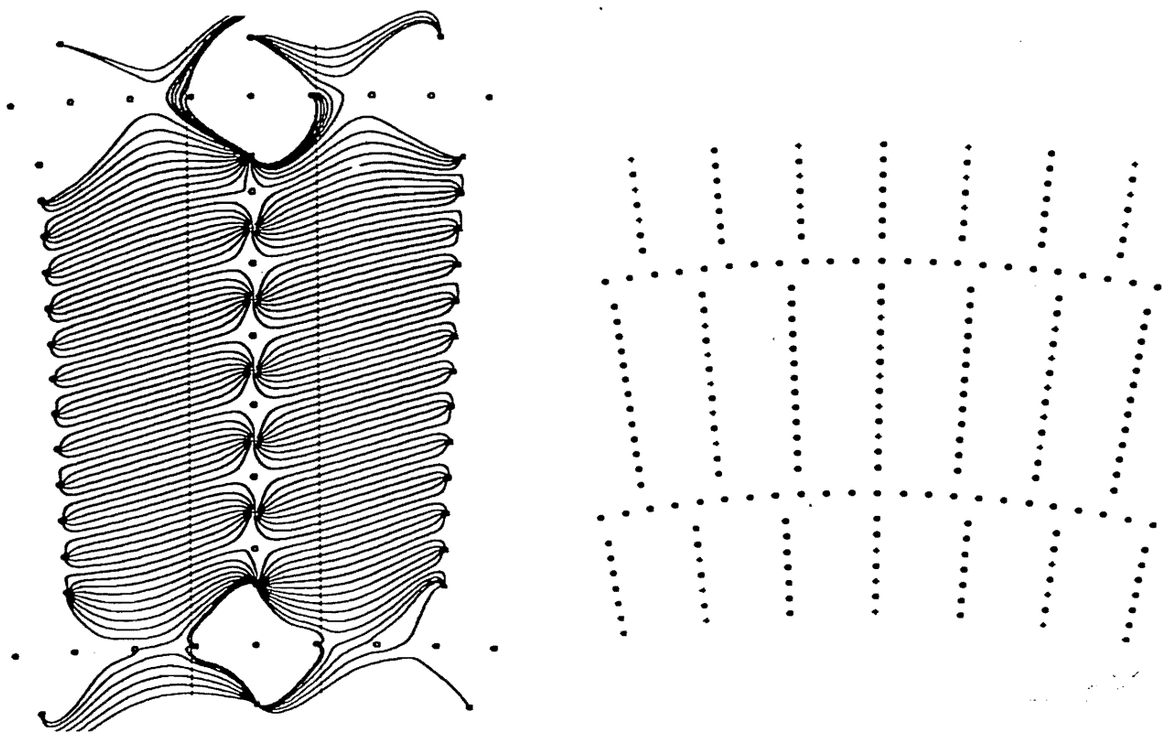

Figure 7: Jet cell geometry. (a) Drift trajectories in cells; (b) superlayer layout. From Ref. [2].

minimize that wasted space by having only a few such spaces between superlayers. Of course, small cells can also be arranged in superlayers.

- Many fewer wires need to be strung, and they could be strung in groups.

### 3.3 Summary on cell geometry

A comparison of small and jet cell designs in a $B$ factory drift chamber is given in Table 3. Most of the problems listed for both small and jet cells are manageable, and only require careful engineering. Perhaps the only fundamental issue is that of diffusion. Diffusion ultimately limits the position resolution in most jet cells, while it can be minimized in small cells. For this reason, most $B$ Factory tracking groups are opting for the small cell design.

## 4 HERMETICITY

Perhaps the most important improvement of a $\tau c$F central tracking system over previous generations of collider detectors is the uniformity of response, large solid angle coverage, and hermeticity down to $|\cos\theta| < 0.95$ (see Fig. 6). These properties continue into the particle ID system, the calorimeter, and the HCAL. The high efficiency

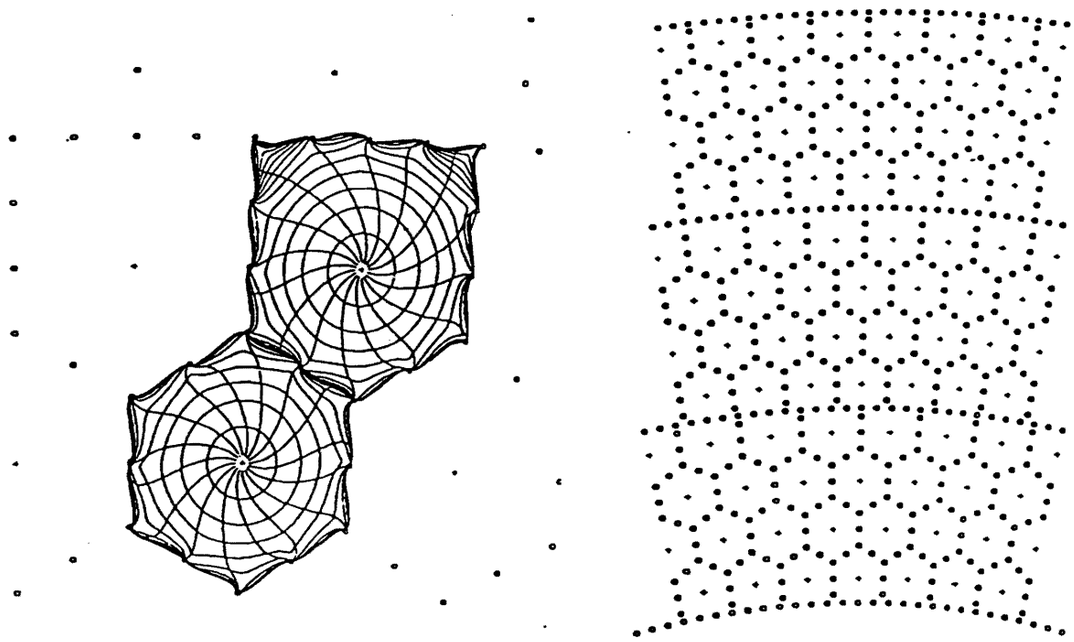

Figure 8: Small (hexagonal) cell geometry. (a) Drift trajectories in cells; (b) superlayer layout. From Ref. [2].

and model-ability of this uniformity is the key to *precision* measurements of dominant processes and *minimal* detector backgrounds for rare processes.

As more realistic machine engineering progresses, one is faced with the problem of supporting the final focussing systems. We have heard in this workshop of plans to make use of a support tube, running straight through the detector at a radius of around 40 or 50 cm, to hold the quads. This would be very similar to the SLAC $B$ Factory design. In this scheme, the central tracking system would be broken into two separate chambers, one at small and one at larger radius. Even if the support tube and chamber walls are made as thin as possible, this would have a negative impact on hermeticity and uniformity of response. If indeed such a support tube is needed, it will be critical to study its impact on the tracking system and on physics analyses. It may turn out that the impact can be made negligible; but it would be a pity to discover, through data analysis, that systematic errors in the drift chamber performance modelling limit our ability to fully exploit the high luminosity of the $\tau c$F.

Table 3: Parameters for a small-cell and a jet-cell drift chamber design for a $B$ Factory (from Ref. [2]).

| Comparison of Cell Designs | | |
|---|---|---|
| Configuration | Small Cell | Jet Cell |
| Number of samples | 39 | 40 |
| Sample size (mm) | 15.0 | 9.0 |
| Half cell width (mm) | 7.5 | 25.0 |
| $\lvert\cos\theta\rvert$ coverage | $< 0.965$ | $< 0.951$ |
| Min forward angle | 15.5° | 17.7° |
| Number of sense wires | 6999 | 2885 |
| Number of field wires | 24997 | 15027 |
| Total Wires | 31996 | 17912 |
| Total $X_0$ from, | | |
| Cu field wires | .0027 | .0032 |
| (Mg field wires) | (.00026) | (.00031) |
| Tungsten sense wires | .00023 | .00008 |
| He-based gas | .00083 | .00083 |
| Total radiation lengths | .0037(.0013) | .0041(.0012) |
| Critical tension ($N$) | 0.027 | 0.14 |

| Comparison of Cell Designs | | |
|---|---|---|
| Configuration | Small Cell | Jet Cell |
| $dE/dx$ | | |
| Resolution (%) | 6.2 | 6.9 |
| Plateau/minimum | 1.46 | 1.43 |
| Separation ($\sigma$) | | |
| $e/\pi$ $p < 0.6$ | 6.6 | 6.2 |
| $p = 1.0$ | 6.0 | 5.5 |
| $p = 2.0$ | 4.3 | 4.0 |
| $p = 4.0$ | 3.0 | 2.8 |
| $K/\pi$ $p < 0.6$ | $< 4.0$ | $< 3.8$ |
| $p = 1.0$ | 0.0 | 0.0 |
| $p = 2.0$ | 2.2 | 2.1 |
| $p = 4.0$ | 2.3 | 2.1 |

## 5 SUMMARY

Drift chamber technology is already fairly mature, and much progress is being made on improving on current designs. Given the constraints on real estate available to a central tracker at a $\tau c$F, it should be possible to design and build a chamber (or set of chambers) which can meet the demands of the physics program. However, certain critical design issues (presence of support tube, cell geometry, endplate design, *etc.*) should be carefully studied, and decisions made as soon as possible, to ensure the quality of the $\tau c$F detector. One of the most useful tools in this study will be the Sevilla GEANT-based Monte Carlo, and its use is strongly encouraged.

## 6 ACKNOWLEDGEMENTS

I have drawn heavily on the work of the SLAC $B$ Factory tracking group. I thank the organizers for a stimulating and pleasant Workshop.

## References


[1] "Central Tracking Design for a $\tau$-Charm Factory", A.J. Weinstein, in *Proceedings of the Tau Charm Factory Workshop*, May 1989, SLAC-343, p. 911.

[2] "Report of the Charged Particle Tracking Group", A. Boyarski, P. Burchat, M. King and A. Weinstein, in *Workshop ... B Factory at SLAC*, March 1991, SLAC-373, p. 379; "Drift Chamber Status Report", A. Boyarski and P. Burchat, *BaBar* Note 76, January 1992; "A Low Mass Drift Chamber for the $B$ Factory", A. Boyarski *et al.*, in *B Factories: State of the Art*, April 1992, SLAC-400, p. 437; "Studies of Helium Gas Mixtures in Drift Chambers", A. Boyarski, D. Briggs, P. Burchat and J. Hiser, *Nucl. Inst. Meth.* **A316**(1992) 217; "Studies of Helium Based Drift Chamber Gases for High Luminosity Low-Energy Machines", A. Boyarski, D. Briggs and P. Burchat, *Nucl. Inst. Meth.* **A323**(1992) 267.

[3] "Measurements of Electron Drift Parameters for Helium and $CF_4$-based Gases", J. Va'Vra, P. Coyle, J. Kadyk and J. Wise, *BaBar* Note 104, April 1993.

[4] "Studies of Helium Gas Mixtures as Drift Chamber Gas", C. Grab, in *B Factories: State of the Art*, April 1992, SLAC-400, p. 443; S.M. Playfer *et al.*, *Nucl. Inst. Meth.* **A315**(1992) 494.

[5] "Study of a Drift Chamber Filled with a Helium-Ethane Mixture", S. Uno, in *B Factories: State of the Art*, April 1992, SLAC-400, p. 449.

[6] "Measurement of Spatial Resolutions and Drift Velocities in a Drift Chamber Filled with a Helium-DME Mixture", V. Cindro *et al.*, *Nucl. Inst. Meth.* **A309**(1991) 411.

[7] "Helium Molecular Gas Mixtures for High Resolution Drift Chambers", B. Schmidt and K. Martens, *Nucl. Inst. Meth.* **A317**(1992) 148.